Geo-INQUIRE Transnational Access Project Report: Reconstruction and Numerical Modeling of Historical and Paleo-tsunamigenic landslides in Lake Rupanco, Chile.

Geo-INQUIRE installation: HySEA - Earthquake and landslide generated tsunami simulations (TA2-531-3)

Project title: Reconstruction and numerical modeling of historical and paleo-tsunamigenic landslides in Lake Rupanco, Chile

Transnational access principal investigator: Juan Pablo Quiroga Quezada (Chile)

Project acronym: IALGTLRCH1960

Project report ID: C1-TA2-531-3-6

Transnational access team: Prof. Jorge Macías Sánchez, Prof. Sergio Ortega (Universidad de Málaga (UMA), Spain)

Date of visit: 7 - 21 October 2024

Geo-INQUIRE Virtual Access:

Data/Products:

A scientific paper published in the Landslides Journal (https://doi.org/10.1007/s10346-025-02629-1) and several mentions in social media (https://www.eha.cl/noticia/actualidad/estudio-reconstruye-antiguos-tsunamis-en-el-lago-rupanco-y-advierte-sobre-riesgos-geologicos-en-los-lagos-del-sur-de-chile; https://eos.org/thelandslideblog/lake-rupanco-1; https://sabes.cl/2025/11/05/hay-que-sumar-un-nuevo-riesgo-de-desastres-en-chile-investigacion-devela-peligrosidad-de-tsunamis-en-los-lagos-del-sur/; https://www.instagram.com/p/DP2AuU1klg0/)

Project report:

The objective of this study was to characterize and model landslides and the resulting tsunamis triggered by the Great 1960 Valdivia earthquake. The main approach involved a field expedition to assess the areas affected by the 1960 landslides, together with the acquisition of a high-resolution bathymetric map of the study area. Through visual inspection of the bathymetric data, in addition to deposits potentially associated with the 1960 landslides, a larger deposit was identified, likely related to an older, pre-1960 landslide and consistent with the currently visible scarp.

Based on these observations, the research team decided to investigate two scenarios: (1) multiple shallow landslides associated with the 1960 event, and (2) a single deep-seated, rotational landslide of larger volume associated with an older event (referred to as PLS3).

Following prior discussions between the principal investigator and Professor Jorge Macías, it was agreed to use the Landslide-HySEA model. These discussions also led to the introduction of the Transnational Access program. After an extensive but successful application process, the principal investigator (Juan Pablo Quiroga) was able to carry out an in-person research stay at the University of Málaga, Spain, where he received direct training on the Landslide-HySEA model, including both its physical formulation and technical implementation. In addition, Juan Pablo gained experience running Landslide-HySEA on the CINECA supercomputing facility in Italy. This combination of factors enabled the execution of a large number of fast and reliable simulations, allowing historical tsunami events in Chile to be reproduced with a high degree of realism.

The geometric characterization was carried out by integrating historical aerial photographs, digital elevation models, historical bathymetry, and a high-resolution bathymetric survey conducted in 2024, complemented by UAV-based photogrammetry and field observations. For the 1960 event, eight source areas (LS1–LS8) were identified, corresponding to shallow, moderate-volume landslides (Fig. 1), whereas the paleo-event was interpreted as a deep-seated, rotational, and coherent landslide with a significantly larger volume (Fig. 2).

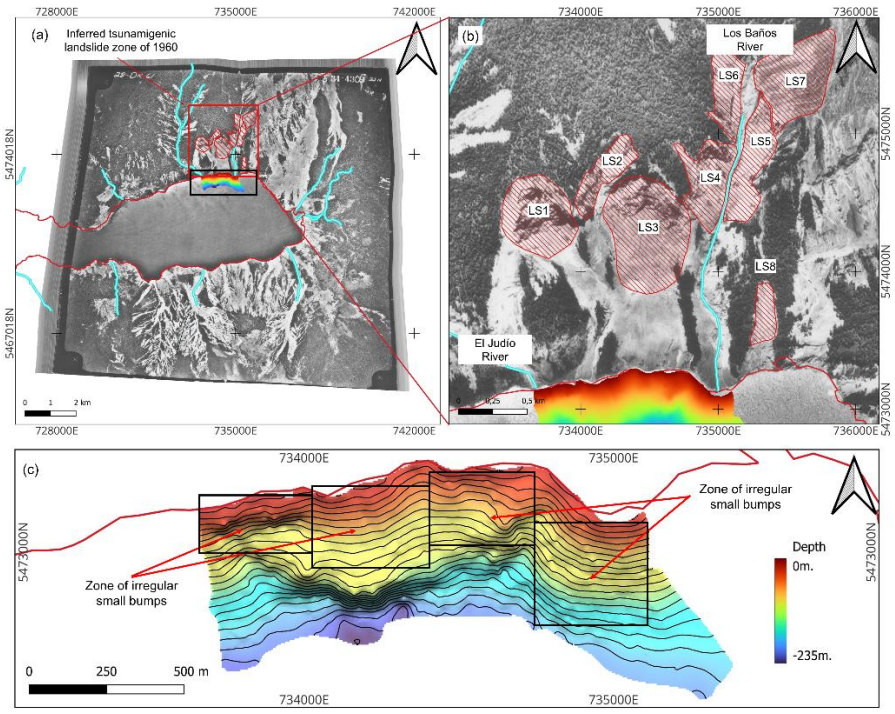

Figure 1: (a) 1961 Historical photograph taken in 1961 by the Instituto Geográfico Militar (IGM). (b) Zoomed-in view of Fig. 1a (red rectangle). Delineation of the 1960 tsunamigenic landslides. (c) Zoomed-in view of Fig. 1a (black rectangle). Delineation of suggested submerged deposits of 1960 landslides, with black rectangles showing the reconstruction zones.

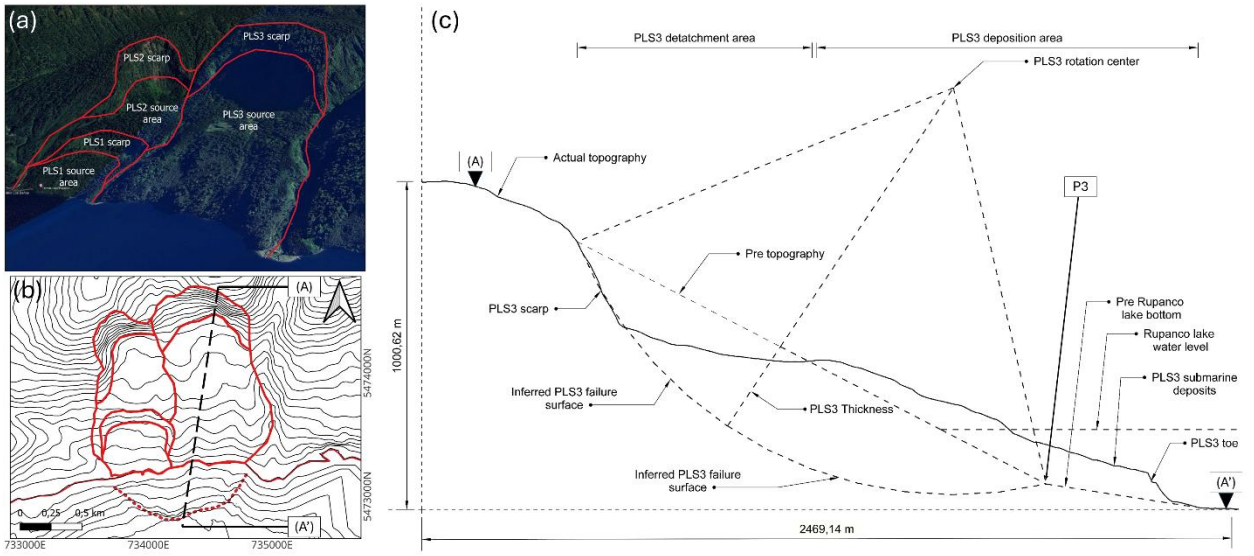

Figure 2: (a and b) Plain view and delimitation of scarps and sources areas of identified paleo-landslides. Black dotted line in Figure b represents elevation profile A-A', and red dotted line represents the end of the large and highly demarcated submarine deposits visible in Fig. 3b. (c) 2D diagram of PLS3 landslide.

Numerical simulations were performed using the Landslide-HySEA model. A 10 m spatial resolution simulation grid including 7.862.706 nodes was employed (Fig. 3). For near-field analysis, only an extent of the lake's eastern side was used (red rectangle), evaluating virtual tide gauges 1 to 3, using a time window of 900 seconds, and a capture interval of 1 second. For far-field analysis, the entirety of the lake was used, evaluating virtual tide gauges 4 to 5, using a time window of 3600 seconds, and a capture interval of 30 seconds.

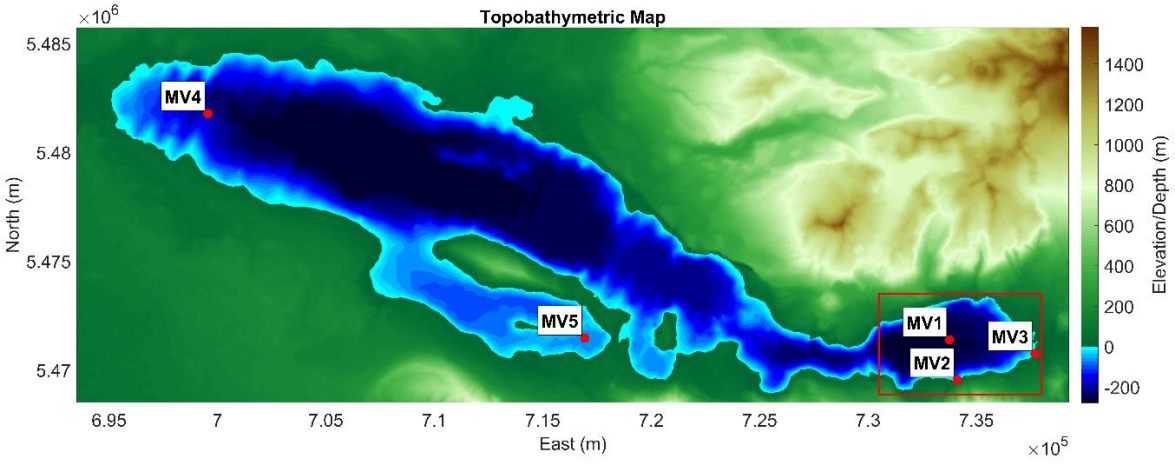

Figure 3: Simulation grid of Lake Rupanco used for tsunami simulations of the 1960 and PLS3 scenarios. The red square indicates the area of interest at its eastern side.

Due to the lack of site-specific geotechnical data, a global sensitivity analysis (GSA) was conducted to systematically identify the most influential rheological parameters and to calibrate the numerical simulations. For the PLS3 paleo-landslide scenario, a total of 35,000 model

realizations were performed, varying four key parameters controlling granular flow and landslide–water interaction: the density ratio between the landslide material and water, the Coulomb friction angle, the interfacial friction coefficient between the granular layer and the water, and the basal Manning roughness coefficient. For the 1960 landslide scenario, the total number of simulations was reduced to 8,000, focusing primarily on the Coulomb friction angle and the initial landslide velocity to account for the effects of strong seismic shaking on landslide initiation and mobility.

The sensitivity analysis demonstrated that the Coulomb friction angle is the dominant parameter controlling landslide mobility, the final submerged landslide volume, and the initial tsunami amplitude in both scenarios. Lower friction angles were associated with increased landslide mobility, larger volumes of material entering the lake, and more energetic tsunami generation, whereas higher friction angles limited landslide runout and reduced wave amplitudes. In contrast, the remaining parameters exhibited comparatively minor influence on the model outputs within the tested ranges, primarily affecting early-stage landslide–water coupling rather than overall tsunami impact. This result highlights the critical role of internal friction in governing tsunamigenic landslide dynamics and provides a physically meaningful basis for parameter calibration in data-limited lacustrine environments. The sensitivity analysis results for the PLS3 scenario can be seen in Figure 4.

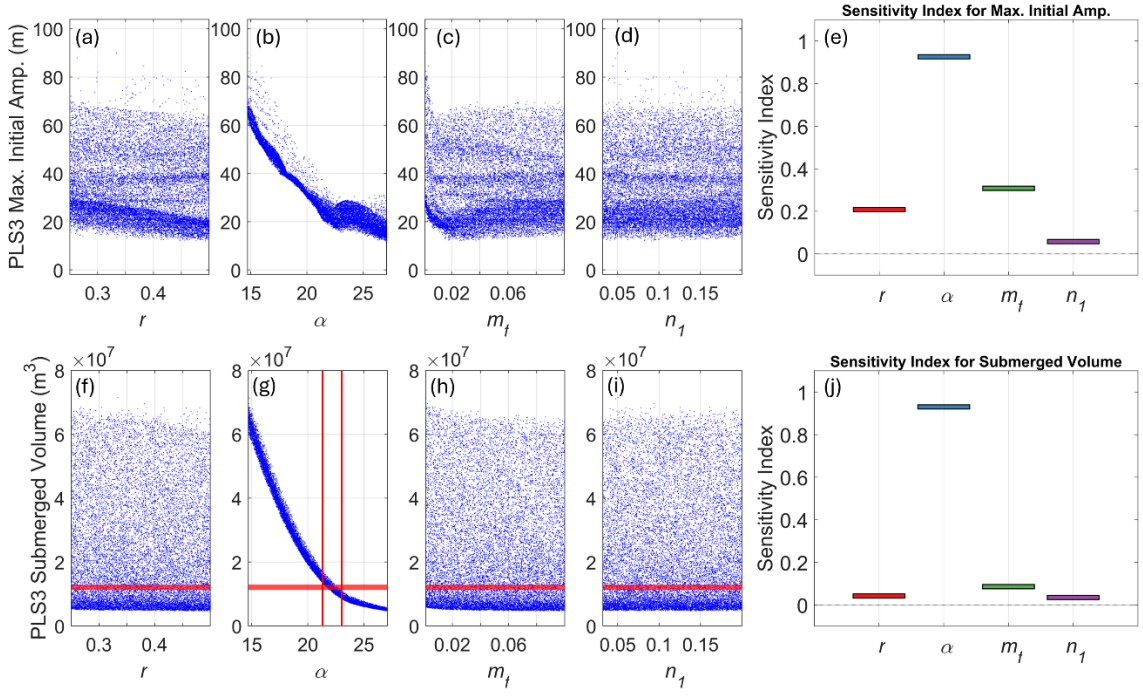

Figure 4: A posteriori parameter distribution for initial maximum tsunami amplitude (a-d) and submerged landslide volume (f-i) for scenario PLS3. Horizontal red lines in plots f to i represent the estimated submerged volume. Vertical red lines represent the minimum (left) and maximum (right) Coulomb friction angles that produce the target PLS3 submerged volume. (e and j) Sensitivity indices associated with each parameter for the two metrics of interest.

The results reveal clear differences between the two scenarios in terms of wave generation, propagation, and inundation patterns. The 1960 event, characterized by multiple fast-moving subaerial landslides impacting the lake in rapid succession, generated complex, multi-peaked wave trains and maximum near-field wave heights of up to 33 m (Fig. 5a). These high amplitudes are primarily associated with the high mobility and initial velocities of the landslides, as well as with the confined geometry of the eastern basin, which promoted constructive wave interference and strong wave focusing. Consequently, the impacts were highly localized, with severe run-up and inundation concentrated along the eastern shoreline, particularly in the Las Gaviotas sector.

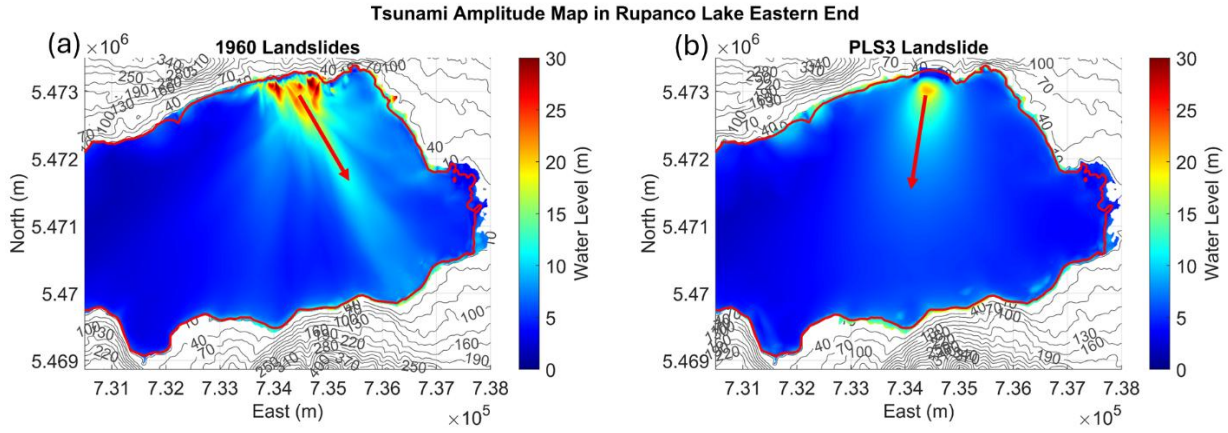

Figure 5: Tsunami amplitude map for both landslide scenarios. (a) 1960 (b) PLS3.

In contrast, the paleo-landslide PLS3, despite its substantially larger volume, generated lower maximum wave heights of approximately 22 m near the source (Fig 5b). This behavior reflects its deeper-seated, more coherent failure mechanism and lower initial acceleration, which resulted in a more gradual momentum transfer to the water column. However, the larger displaced volume and sustained interaction with the lake produced waves with greater spatial persistence, leading to a broader distribution of tsunami energy across the lake basin and more pronounced far-field effects, particularly along the southern shoreline. This can be seen at the virtual tide gauges comparisons. For the 1960 scenario, higher amplitude waves can be seen for virtual tide gauge points near the source area (MV3 in Fig. 6), whereas for virtual tide gauges far from the source area (MV4 and MV5 in Fig. 6), the higher amplitude waves are attributed to the PLS3 scenario, although having an amplitude difference of ~0.1-0.2 m.

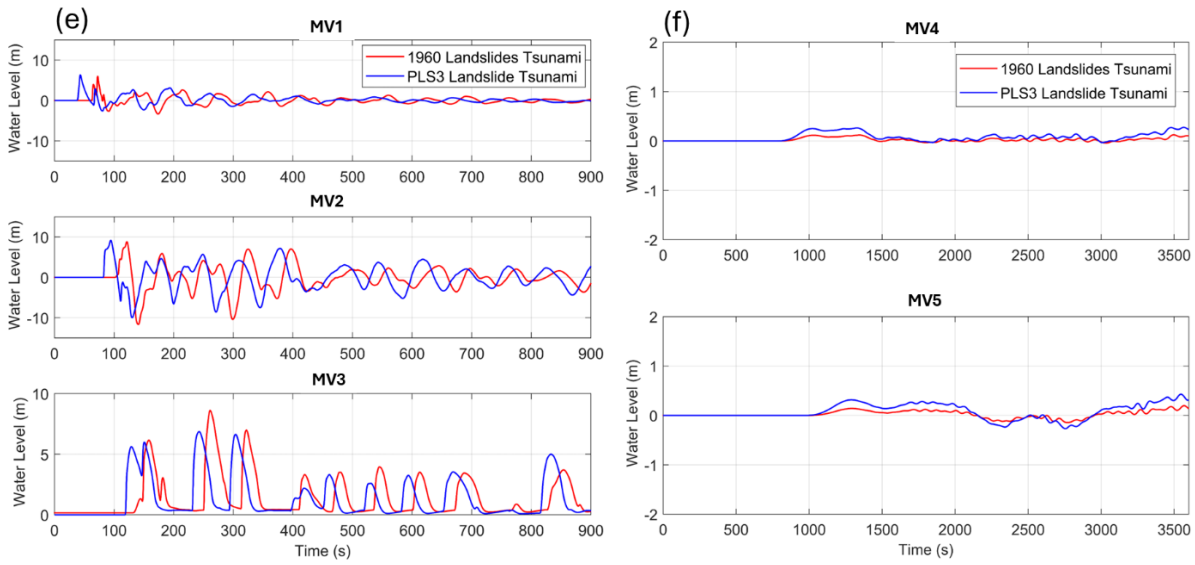

Figure 6: 1960 vs PLS3 virtual tide gauges from near and far field analysis.

Both scenarios resulted in significant inundation at the Las Gaviotas sector. The 1960 scenario reached 286.6 m (horizontal) and 9.5 m (vertical), while PLS3 reached 269 m (horizontal) and 8.5 m (vertical), respectively. The 1960 event produced sharper and more severe inundation in this area, characterized by high flow depths and abrupt inland penetration concentrated near the landslide source. In contrast, the paleo-landslide scenario generated less extreme but more spatially uniform inundation at Las Gaviotas, with lower peak flow depths but a broader lateral distribution along the shoreline.

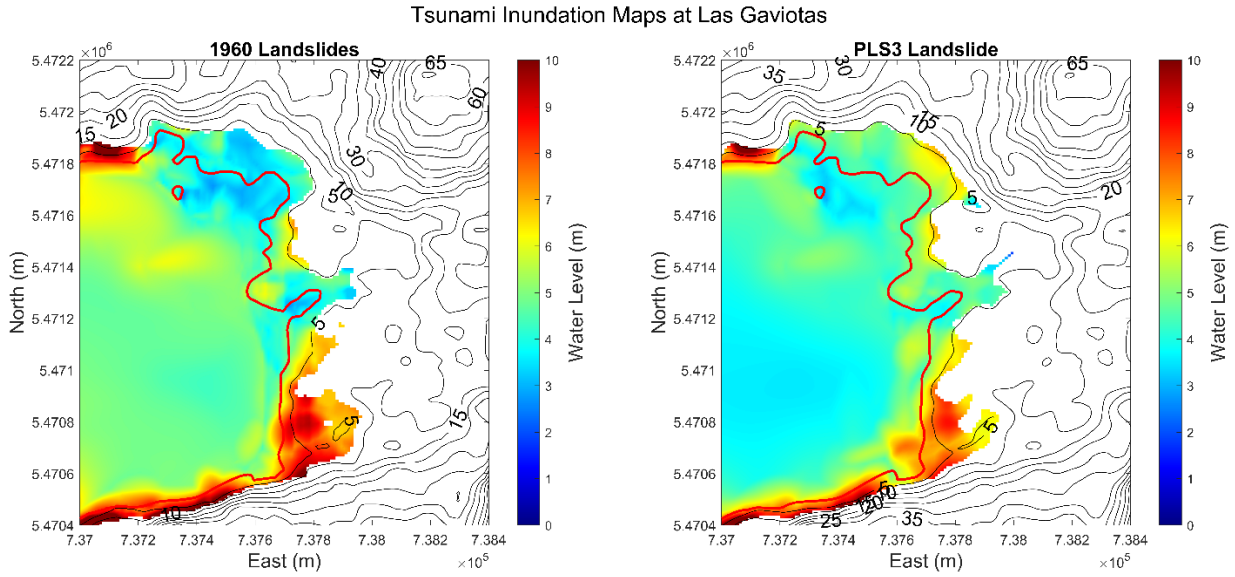

Figure 7: Inundation maps for both tsunami scenarios. (left) 1960 (right) PLS3.

Snapshots of interest can be seen in Figures 8 and 9 for the 1960 and PLS3 scenarios, respectively.

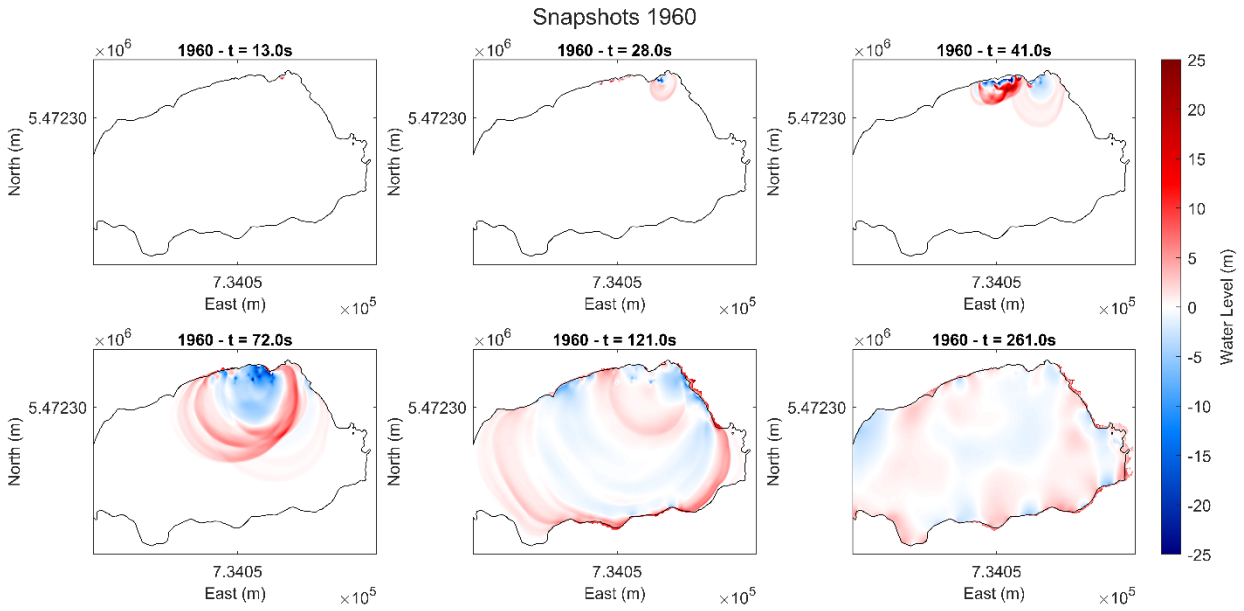

Figure 8: Snapshots of the 1960 tsunami simulation.

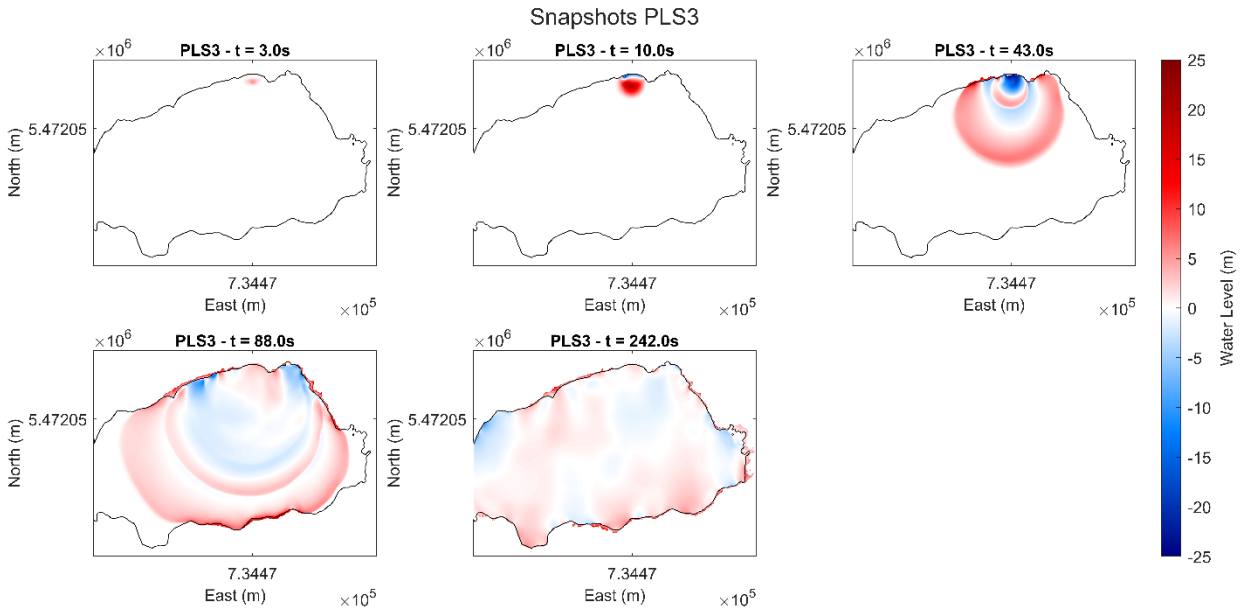

Figure 9: Snapshots of the PLS3 tsunami simulation.

Data supporting this study, such as HySEA parameter text files, tsunami simulation videos, and other figures regarding tsunami analysis for both landslide scenarios are available at ttps://github.com/JuanQuirogaQuezada/Rupanco-HySEA.